AIP | Journal of Applied Physics

Measurements of face shear properties in relaxor-PbTiO3 single crystals

Shujun Zhang, Wenhua Jiang, Richard J. Meyer, Fei Li, Jun Luo et al.

Citation: J. Appl. Phys. **110**, 064106 (2011); doi: 10.1063/1.3638691
View online: http://dx.doi.org/10.1063/1.3638691
View Table of Contents: http://jap.aip.org/resource/1/JAPIAU/v110/i6
Published by the American Institute of Physics.

Measurements of face shear properties in relaxor-$PbTiO_3$ single crystals

Shujun Zhang,[1,a)] Wenhua Jiang,[1] Richard J. Meyer, Jr.,[2] Fei Li,[1,3] Jun Luo,[4] and Wenwu Cao[1]
[1]*Materials Research Institute, Pennsylvania State University, University Park, Pennsylvania 16802, USA*
[2]*Applied Research Lab., Pennsylvania State University, University Park, Pennsylvania 16802, USA*
[3]*Electronic Materials Research Laboratory, Key Lab of the Ministry of Education, Xi'an Jiaotong University, Xi'an 710049, China*
[4]*TRS Technologies Inc., 2820 East College Avenue, State College, Pennsylvania, 16801, USA*

(Received 8 June 2011; accepted 6 August 2011; published online 22 September 2011)

The face (contour) shear piezoelectric properties of $Pb(Mg_{1/3}Nb_{2/3})O_3$-$PbTiO_3$ (PMNT) single crystals were experimentally determined by the impedance method. $Zt \pm 45°$ cut samples with various aspect ratios were investigated based on Bechmann's zero-order approximate solution. Square plates were found to exhibit a clean face shear vibration mode and the experimental data were in good agreement with the rotated matrix calculations and finite element method simulations. The piezoelectric coefficients d_{36} were determined to be in the range of 1600-2800 pC/N, depending on the compositional variations, with an ultralow frequency constant N_{36}, in the range of 490–630 Hz.m. In contrast to conventional thickness shear modes, the mechanical quality factors of face shear vibrations are relatively high, with Q values being on the order of ~100-450, demonstrate promising for low frequency transducer applications. © *2011 American Institute of Physics*.
[doi:10.1063/1.3638691]

I. INTRODUCTION

New application areas for actuator and transducer design continue to be the driving force for the innovations in piezoelectric materials. The piezoelectric coefficient (d_{ij}) and electromechanical coupling (k_{ij}) are the most important parameters for determining device performance.[1] Relaxor-$PbTiO_3$ single crystals, including $Pb(Mg_{1/3}Nb_{2/3})O_3$-$PbTiO_3$ (PMNT), $Pb(Zn_{1/3}Nb_{2/3})O_3$-$PbTiO_3$ (PZNT) and $Pb(In_{0.5}Nb_{0.5})O_3$-$Pb(Mg_{1/3}Nb_{2/3})O_3$-$PbTiO_3$ (PIN-PMN-PT), have been extensively studied in last two decades, due to their superior longitudinal piezoelectric coefficients ($d_{33} > 1500$ pC/N) and electromechanical coupling factors ($k_{33} > 90\%$), when poled along the crystallographic direction [001].[2–6] In addition, [011] poled single crystals offer high extensional piezoelectric and electromechanical properties, with $-d_{32} > 1200$ pC/N and $k_{32} > 85\%$.[7–17] In contrast to [001] poled crystals, longitudinal mode along [011] direction shows high mechanical quality factor $Q \sim 500$, demonstrating good potential for high power applications.[18] Of particular significance for [011] poled crystals is the large face (contour) shear vibration can be achieved in $Zt \pm 45°$ cut samples (as shown in Fig. 1), with piezoelectric coefficient d_{36} being on the order of ~2600 pC/N, equal to the combined values of the two transverse piezoelectric coefficients $d_{36} = d_{31} - d_{32}$.[19] Recently, ultralow frequency sonar transducers were projected based on the face shear d_{36} in PMNT crystals, due to their ultralow frequency constant and high piezoelectric coefficient of this vibration mode.[20,21] Furthermore, the *ac* driving field level and mechanical quality factor Q of the face shear mode were reported to be significantly higher compared to thickness shear vibration modes, owing to the fact that the working electrodes are along the same direction as that of the polarization.[22–24]

The piezoelectric and elastic properties of the face shear vibration in quartz crystals had been extensively studied from 1930s to 1950s. However, the analytic solution for the vibration mode that satisfies displacement equation of motion, as well as all the boundary conditions of free edges, has not yet been obtained up to date. Various approximate solutions for the displacement field and resonance frequencies were proposed.[25–28] Bechmann[27] used the zero-order approximate perturbation solutions proposed by Ekstein[28] to describe the contour vibration modes of rotated Y-cut plate resonators. It was found that the calculations based on the zero-order perturbation solutions were in good agreement with the experimental results. After some corrections, those approximate formulas are recommended in IRE Standard on piezoelectric crystals.[25] For relaxor-PT crystals, however, the piezoelectric coefficient was found to be three orders of magnitude higher than that of quartz crystals; thus, it is important to see if the approximation is still plausible for the case of high performance relaxor-PT single crystals.

In this study, the resonance and anti-resonance frequencies of the face shear vibration mode were measured by the impedance method. PMNT crystals with square plate dimensions were used, where the elastic compliance s_{66}^E, electromechanical coupling factor k_{36} and piezoelectric coefficient d_{36} were calculated using Bechmann's zero-order approximate formulae. Simulations using ATILA finite element package were also made to verify the analytical conclusions.

II. CALCULATIONS

Rhombohedral PMNT single crystals possess the macroscopic symmetry *mm2* when poled along the crystallographic [011] direction. According to the IRE standard,[25] the Z axis

a)Author to whom correspondence should be addressed. Electronic mail: soz1@psu.edu.

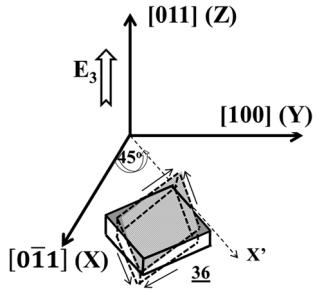

FIG. 1. Schematic of *Zt 45°* - cut sample, and related face shear piezoelectric deformation.

is the poling direction [011], X axis is along [0$\bar{1}$1] direction thus the Y axis is along [100], forming a right-hand orthogonal coordinate system, as shown in Fig. 1.

Table I shows the matrix of elastic compliance s^E, piezoelectric strain coefficient d_{ij} and dielectric permittivity ε_r of [011] poled PMNT28 crystals in the original coordinates, where the high extensional piezoelectric d_{32} and thickness shear piezoelectric d_{15} were found to be on the order of -1188 and 1630 pC/N, respectively. The transformed matrix was obtained by a Zt 45° rotation. The elastic, piezoelectric and dielectric permittivity after rotation are given in the same Table, where the face shear vibration related elastic compliance s_{66}^E and piezoelectric d_{36} were calculated according to the following equations:

$$s'_{66} = s_{11} + s_{22} - 2s_{12}, \tag{1}$$

$$d'_{36} = \pm(d_{32} - d_{31}), \tag{2}$$

with the values found to be on the order of 120 pm^2/N and −1648 pC/N, respectively. For convenience, we used absolute values for the piezoelectric coefficients in the following.

In the rotated coordinate, the electrode face of the sample is normal to 2-fold symmetric axis, the other edges of the samples are along rotated X′ and Y′ axes. Under the assumption of the infinitely thin plate, the following zero-order approximate formulae are used to extract the face-shear materials properties of PMNT single crystals, based on the impedance measurements.

The frequency constant of the face shear vibration for a square plate sample can be calculated by

$$N_{36} = f_r \cdot l = \frac{F}{2}\sqrt{\frac{1}{\rho s_{66}^E}}, \tag{3}$$

from the measured resonance frequency, the elastic compliance of the face shear vibration can be determined by

$$s_{66}^E = \frac{F^2}{4\rho(f_r 1)^2} \tag{4}$$

where l is the edge length of the plate. F is a correction constant with value equal to $F = \frac{2\kappa_0\alpha}{\pi}$, where $\kappa_0 = 2.0288$, the first root of the transcendental equation $\kappa + \tan\kappa = 0$ and $\alpha = 1 - 0.05015 \times [(s_{11}^E + s_{22}^E)/2s_{66}^E]^{1/2}$. In the Zt ± 45° rotated *mm2* matrix, $s_{11}^E = s_{22}^E \ll s_{66}^E$, thus $\alpha \cong 1$.

The electromechanical coupling factor is given by

$$k_{36}^2 = \frac{1}{1 + rp}, \tag{5}$$

where p is a correction constant, $p = 4\alpha^2 b/(\kappa_0^2 + 2)$ with $b = 1 - 0.0691 \times [(s_{11}^E + s_{22}^E)/2s_{66}^E]$. As mentioned above, $s_{11}^E = s_{22}^E \ll s_{66}^E$, thus $b \cong 1$.

In Eq. (5), r is the capacitance ratio ($r = \frac{c_o}{c_1}$: C_0 is the shunt capacitance and C_1 the motional capacitance), the reciprocal of which is related to the measured resonance and anti-resonance frequencies:

TABLE I. Full matrix of material constants for [011] poled PMNT28 crystals, including elastic compliances (a), piezoelectric strain coefficient (b) and dielectric permittivity (c), before and after *Zt 45°* -rotation.

$$\begin{bmatrix} 14.4 & -23.6 & 15.5 & 0 & 0 & 0 \\ -23.6 & 58.1 & -37.6 & 0 & 0 & 0 \\ 15.50 & -37.6 & 30.5 & 0 & 0 & 0 \\ 0 & 0 & 0 & 14.7 & 0 & 0 \\ 0 & 0 & 0 & 0 & 101 & 0 \\ 0 & 0 & 0 & 0 & 0 & 18.8 \end{bmatrix} \overset{zt\ 45^\circ\ rotation}{\Leftrightarrow} \begin{bmatrix} 11.0 & 1.64 & -11.0 & 0 & 0 & 21.9 \\ 1.64 & 11.0 & -11.0 & 0 & 0 & 21.9 \\ -11.0 & -11.0 & 30.5 & 0 & 0 & -53.8 \\ 0 & 0 & 0 & 57.7 & -43.0 & 0 \\ 0 & 0 & 0 & -43.0 & 57.7 & 0 \\ 21.9 & 21.9 & -53.8 & 0 & 0 & 120 \end{bmatrix} \quad \text{(a)}$$

$$\begin{bmatrix} 0 & 0 & 0 & 0 & 1630 & 0 \\ 0 & 0 & 0 & 239 & 0 & 0 \\ 460 & -1188 & 890 & 0 & 0 & 0 \end{bmatrix} \overset{zt\ 45^\circ\ rotation}{\Leftrightarrow} \begin{bmatrix} 0 & 0 & 0 & -696 & 935 & 0 \\ 0 & 0 & 0 & 935 & -696 & 0 \\ -364 & -364 & 890 & 0 & 0 & -1648 \end{bmatrix} \quad \text{(b)}$$

$$\begin{bmatrix} 6410 & 0 & 0 \\ 0 & 1470 & 0 \\ 0 & 0 & 3800 \end{bmatrix} \overset{zt\ 45^\circ\ rotation}{\Leftrightarrow} \begin{bmatrix} 3940 & -2470 & 0 \\ -2470 & 3940 & 0 \\ 0 & 0 & 3800 \end{bmatrix} \quad \text{(c)}$$

$$\frac{1}{r} = \frac{f_a^2 - f_r^2}{f_r^2} = \frac{\beta F^2}{4}\left(\frac{d_{36}^2}{\varepsilon_{33}^m s_{66}^E}\right), \tag{6}$$

where $\beta = \frac{4\pi^2 b}{\kappa_0^2(\kappa_0^2+2)}$, $\varepsilon_{33}^m = \varepsilon_{33}^T - \frac{d_{36}^2}{s_{66}^E}$, from which the face shear piezoelectric coefficient can be determined according to the equation

$$d_{36}^2 = \frac{\varepsilon_{33}^T s_{66}^E}{1+rp} = k_{36}^2 \varepsilon_{33}^T s_{66}^E. \tag{7}$$

The mechanical quality factor Q_{36} for the face shear mode was evaluated by the 3dB method:

$$Q = \frac{f_r}{f_2 - f_1}, \tag{8}$$

where f_r is the resonance frequency, f_2 and f_1 are frequencies at 3dB down from the maximum admittance.

III. EXPERIMENTAL

The PMNT crystals used in this study were grown by the modified Bridgman method along the crystallographic [001] direction. The crystals were oriented using real-time Laue X-ray system. Zt ± 45° cut [011] oriented PMNT crystal samples with different aspect ratios, from 20:2:1 to 10:10:5, were prepared. All the samples were poled at a field of 10 kV/cm at room temperature. The capacitance and dielectric loss were determined using an HP4284A multi-frequency *LCR* meter, while the resonance and anti-resonance frequencies were measured using an HP4294A Impedance phase-gain analyzer.

IV. RESULTS AND DISCUSSION

In order to get clean face shear vibration mode, PMNT crystal samples with various aspect ratios were studied. First, the length/thickness ratio was kept constant, while the length/width ratio was varied. The impedance characteristics as a function of frequency and length/width ratio for PMNT29 crystals were shown in Fig. 2. For a bar shaped sample with dimension of 10 mm × 2 mm × 0.5 mm, a strong vibration was found to occur at 131.5 kHz, with a small vibration observed at lower frequency of 95 kHz, while for square plate of 10 mm × 10 mm × 0.5 mm, two strong peaks were found at 131 kHz and 57 kHz, respectively. The peak at ~131kHz was related to the resonance frequency of extensional vibration in the bar samples, it should be noted that extensional vibration remains in square plate, due to the fact that the acoustic velocities along X- and Y-directions are the same in Zt ± 45° cut samples ($s_{11} = s_{22}$). Of particular significance is that a clean face shear vibration can be achieved in square plates with dimension of 10 mm × 10 mm × 0.5 mm. Thus, the elastic compliance, electromechanical coupling factor and piezoelectric coefficient of PMNT29 were calculated according to Eqs. (4), (5), and (7), and found to be on the order of 159 pm^2/N, 0.81, and 2030 pC/N, respectively. According to Eq. (2), the face shear piezoelectric d_{36} was on the same order of $d_{31} - d_{32}$, thus, *ZX*- and *ZY*- cut PMNT29 samples with the same composition were

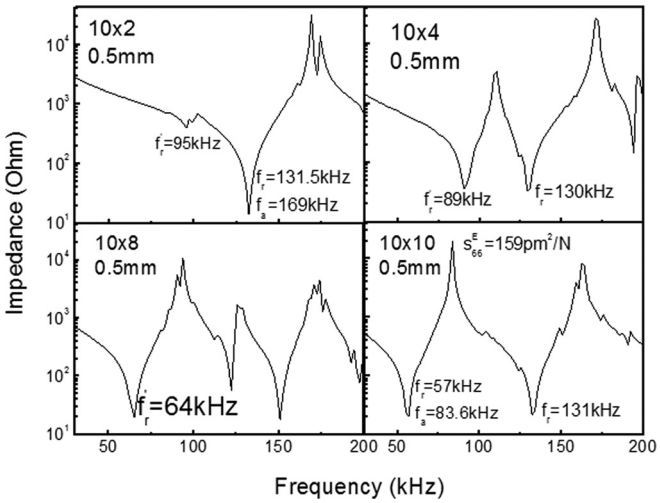

FIG. 2 Impedance characteristics as a function of frequency for PMNT29 crystals with different aspect ratios.

fabricated, from which the extensional piezoelectric d_{31} and d_{32} were measured and found to be 540 pC/N and − 1530 pC/N, respectively. The calculated d_{36} was found to be on the order of 2070 pC/N, very close to the measured value of 2030 pC/N, as listed in Table II. This in turn, demonstrated the suitability to use square plate in face shear mode for the determination of face shear piezoelectric coefficient of high performance relaxor-PT crystals, based on the formulae listed in the preceding section.

For a rectangular plate, Eq. (3) is changed to

$$f_r = \frac{F}{a+b}\sqrt{\frac{1}{\rho s_{66}^E}}, \tag{9}$$

where *a* and *b* are the length and width of the plate, respectively. The calculated resonance frequencies of the face shear vibration for the plate samples with the dimensions of 10 mm × 2 mm × 0.5 mm, 10 mm × 4 mm × 0.5 mm, and 10 mm × 8 mm × 0.5 mm by using Eq. (9) are 95 kHz, 81 kHz, and 63 kHz, respectively, which are very close to the measured ones, as shown in Fig. 2. The anti-resonance frequencies of the bar-shape samples, however, were found to be strongly coupled with the extensional vibration, only samples with square plate shape exhibit clean face shear vibration mode.

For the square plate samples, the effect of the edge length was further investigated and the impedance characteristics are presented in Fig. 3. Clean face shear vibrations were obtained regardless of the edge length of the square

TABLE II. Extensional and face shear properties of [011] poled PMNT29 crystals.

Dimension	ij	K_{ii}	N_{ij} (Hz m)	s_{ij}^E (pm^2/N)	k_{ij}	d_{ij} (pC/N)
10 × 2.0 × 0.5	31 (*ZX*-cut)	4500	1430	15.1	0.70	540
10 × 2.0 × 0.5	32 (*ZY*-cut)	4500	640	75.9	0.88	−1530
10 × 10 × 0.5	36 (*Zt* ± 45° - cut)	4500	570	159	0.81	2030
$d_{36} = d_{31} - d_{32} = 2070$ pC/N; Error ~ 2%						

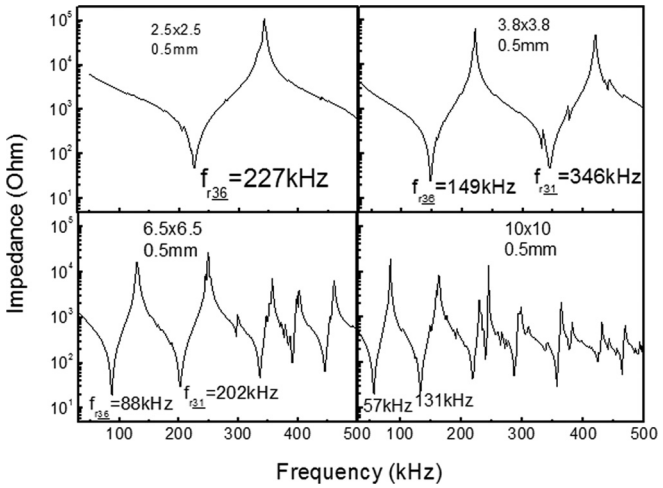

FIG. 3 Impedance characteristics as a function of frequency for square plate PMNT29 samples with different lengths.

plates. The resonance frequency was found to shift downward with increasing the length of the samples, with the same frequency constant N_{36}, being on the order of ~570Hz m.

Fig. 4 shows the impedance characteristics of $Zt \pm 45°$ -cut square plate PMNT28 crystals as a function of sample thickness. Two strong vibrations are observed for samples with $4 \times 4 \times 0.5 \sim 2$ mm^3 dimensions in the frequency range of 100-450 kHz, associated with the face shear vibration at a lower frequency and extensional vibration at a higher frequency, however, three vibrations are found in the cubic sample with the dimensions of $4 \times 4 \times 4$ mm^3, related to the face shear and extensional (longitudinal and lateral) vibration modes, respectively. The detailed face shear properties are listed in Table III. The dielectric permittivity, electromechanical coupling, piezoelectric coefficient and elastic compliance were found to be on the order of 3800, 0.77, 1600 pC/N, and 127 pm^2/N, respectively. The variations of the piezoelectric and elastic compliance are in the range of 3%-4% compared to the calculated values using matrix rotation, as listed in Table I. The measured coupling factor, ~0.77,

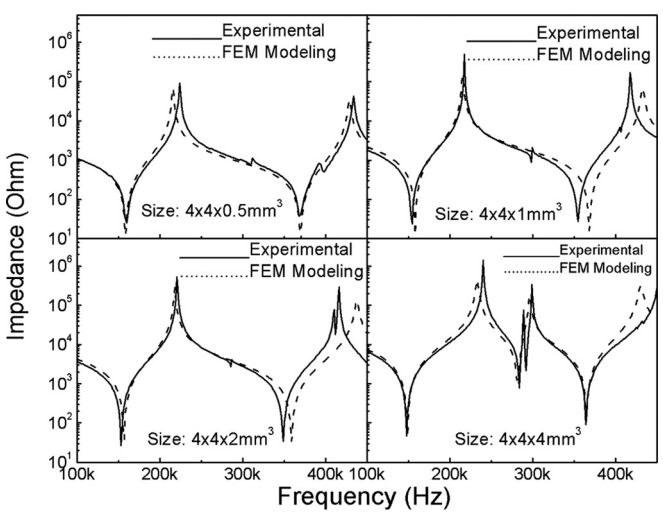

FIG. 4 Impedance characteristics as a function of frequency for square plate PMNT28 samples with different thicknesses. The dashed lines are the ATILA FEM simulation results.

TABLE III. Properties of $Zt \pm 45°$ *-cut* PMNT28 square plate crystals with different thickness.

Dimension	$\varepsilon_{33}^T/\varepsilon_0$	k_{36}	d_{36} (pC/N)	s_{66}^E (pm2/N)	N_{36} (Hz m)	Q_{36}
$4 \times 4 \times 0.5$	3800	0.77	1600	127	637	170
$4 \times 4 \times 1$	3800	0.78	1650	133	620	200
$4 \times 4 \times 2$	3800	0.79	1700	138	610	350
$4 \times 4 \times 4$	3800	0.85	1880	145	595	450

was slightly lower than the static coupling factor, ~0.82, calculated directly by $k_{36} = d_{36}/\sqrt{\varepsilon_{33}^T s_{66}^E}$, which may be due to the assumptions made in the zero-order approximation do not exactly meet in the present experiments.

The coupling factors, piezoelectric coefficients and elastic compliances were found to increase with increasing sample thickness, as summarized in Table III. In order to understand this phenomenon, finite element method (FEM) modeling was performed using ATILA, with input from the original matrix data given in Table I. The FEM modeling results are in good agreement with the experimental measurements, as shown in Fig. 4. Fig. 5 shows the FEM modeling results of the impedance as a function of sample thickness, the resonance frequencies of the face shear vibration were found to maintain similar values, ~158 kHz, for samples with $4 \times 4 \times 0.5 \sim 2$ mm^3 dimensions. The antiresonance frequencies slight increase with increasing sample thickness. Thus, the calculated electromechanical coupling factors show a slight increase with thickness (~0.77-0.79), using Eq. (5). However, for the cubic sample, the resonance frequency was found to shift downward, while the antiresonance frequency shift upward due to the strong coupling of the face shear to the longitudinal vibration mode. A much higher electromechanical coupling factor, ~0.85, was obtained using Eq.(5), which is obviously unphysical. In general, the coupling factor will decrease when the vibrations are strongly coupled,[29] in which case, the zero-order approximate solution is no longer valid, and Eq. (5) cannot be used for coupling calculation. Therefore, further theoretical investigation on the dynamic coupling k_{36} for coupled mode situation is required.

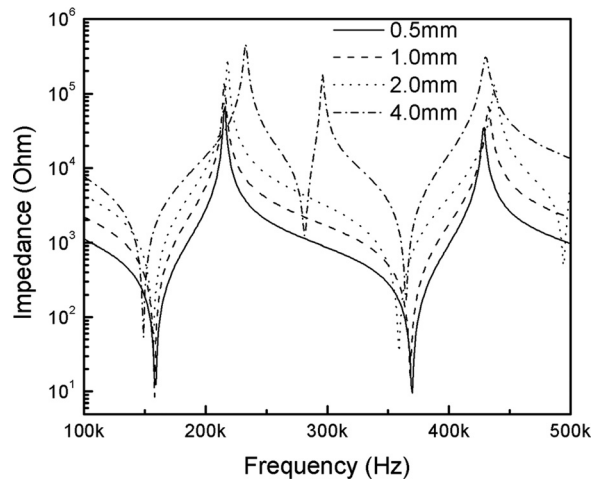

FIG. 5 FEM simulated impedance characteristics for square plate PMNT28 samples with different thicknesses.

In order to check the purity of the face shear vibration in thin square plate, the deformation shapes of the $4 \times 4 \times 0.5$ mm^3 sample were modeled by FEM at the resonance frequencies of 158 kHz and 370 kHz, corresponding to the face shear and extensional vibrations, respectively, as shown in Figs. 6(a) and 6(b). The dark red color stands for the highest positive Y-displacement, while the dark blue color represents the highest negative Y- displacement. Obviously the deformation shape in Fig. 6(a) exhibits a typical pure face shear vibration. However, the deformation shape indicted in Fig. 6(b) shows three displacement nodes which mean there may be a strong coupling between the extensional vibration and the third harmonic of the face shear mode. Therefore, the extensional mode is not a pure clean one. This coupling becomes stronger as the thickness increases and will affect the anti-resonance frequency of the face shear mode, which makes the zero-order approximation invalid.

The face shear properties as a function of composition in PMNT system was also investigated and the results are summarized in Table IV. For PMNT crystals with rhombohedral composition, the Curie temperature was found to increase with increasing the PT content, while the ferroelectric phase transition temperature (including rhombohedral to tetragonal or rhombohedral to orthorhombic phase transition) was decreased, due to the curved morphotropic phase boundary (MPB). The face shear dielectric, elastic, piezoelectric and electromechanical properties were found to increase with decreasing the ferroelectric phase transition temperature, following the general trend observed in relaxor-PT crystals.[3] The mechanical quality factor, however, was found to decrease as the composition approaching the MPB, due to easier polarization rotation. Of particular significance is that the mechanical Q value is higher than those observed in the thickness shear mode (~30).[23] With further increasing PT content, the PMNT crystal was found to be in orthorhombic phase, and becomes single domain state when poled along [011] direction. Thus, the dielectric and piezoelectric properties deteriorate greatly, but the mechanical Q is enhanced, being on the order of ~400.

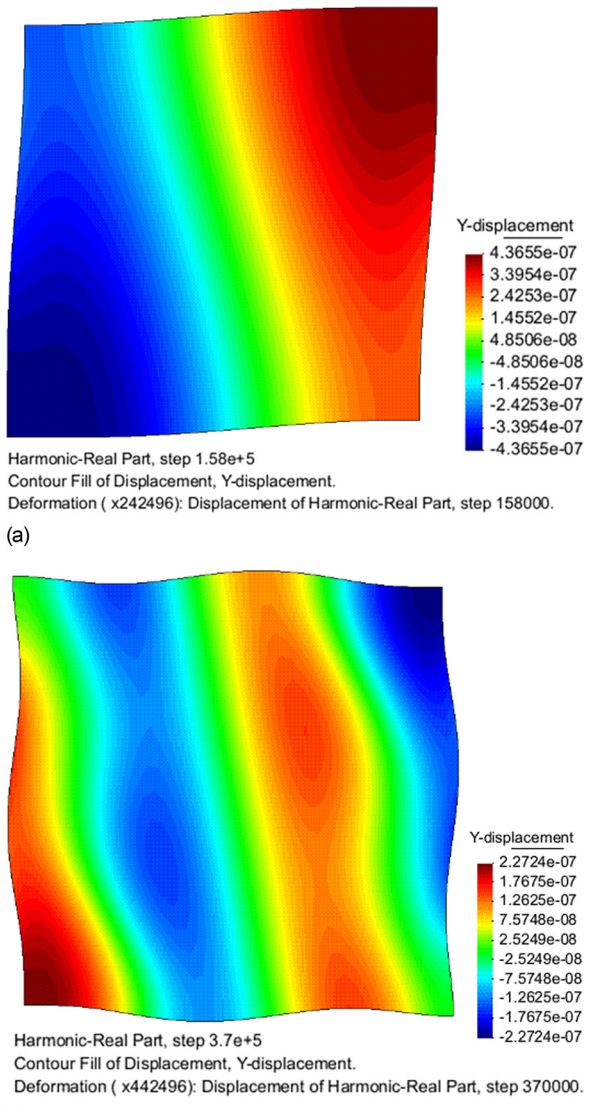

FIG. 6 (Color online) (a) The deformation shape of a thin square plate PMNT28 sample, modeled by FEM at 158 kHz, (b) the deformation shape of a thin square plate PMNT28 sample, modeled by FEM at 370 kHz.

TABLE IV. Properties of $Zt \pm 45°$ *-cut* PMNT crystals with various compositions (4 mm × 4 mm × 0.5 mm).

PMNT	T_C (°C)	T_{FF} (°C)	$\varepsilon_{33}^T/\varepsilon_0$	k_{36}	d_{36} (pC/N)	s_{66}^E (pm2/N)	N_{36} (Hz m)	Q_{36}
PMNT28	128	100	3800	0.77	1600	127	637	170
PMNT28.5	131	95	4300	0.78	1730	129	630	150
GPMNT29	133	90	4500	0.81	2030	159	570	130
PMNT30	138	70	5800	0.83	2800	225	490	100
PMNT32	150	80	1000	0.56	300	37	1200	400

V. CONCLUSION

In conclusion, using thin square plate samples, the properties of the face (contour) shear vibration mode of high performance PMNT single crystals was evaluated using the impedance method based on the formulae under the zero-order approximation. The experimental results are in good agreement with the matrix rotation calculation and the FEM simulation. The errors are only about 3-4%, demonstrating the feasibility of the approximation for the determination of face shear properties of relaxor-PT crystals. The high piezoelectric coefficient, d_{36}, in the range of 1600-2800 pC/N, together with the ultralow frequency constant, N_{36} ~490-640 Hz m, and high mechanical quality factor, make the face shear vibration mode of relaxor-PT crystals excellent candidate for low frequency transducer applications. In addition, the thickness dependence of the electromechanical coupling factor k_{36} for the square resonators revealed the limitation of the zero-order approximation. It is desirable for future theoretical investigations on the dynamic electromechanical coupling factor, when there are strong mode couplings in the face shear resonators.

ACKNOWLEDGMENTS

The authors thank to Prof. T. R. Shrout for his valuable discussion. The work supported by ONR.

[1]T. Shrout, R. Eitel, and C. Randall, "High performance, high temperature perovskite piezoelectric ceramics," in *Piezoelectric Materials in Devices*, edited by N. Setter, (Lausanne, Switzerland, 2002) pp. 413–432.
[2]S.-E. Park and T. R. Shrout, J. Appl. Phys. **82**, 1804 (1997).
[3]S. J. Zhang, T. R. Shrout, IEEE Trans. Ultrason. Ferroelectr. Freq. Contr. **57**, 2138 (2010).
[4]H. Luo, G. Xu, H. Xu, P. Wang, and Z. Yin, Jpn. J. Appl. Phys. **39**, 5581(2000).
[5]D. Damjanovic, IEEE Trans. Ultrason. Ferroelectr. Freq. Contr. **56**, 1574 (2009).
[6]F. Li, S. Zhang, Z. Xu, X. Wei, J. Luo, and T. Shrout, J. Appl. Phys. **108**, 034106 (2010).
[7]Y. Y. Zhang, D. A. Liu, Q. H. Zhang, W. Wang, B. Ren, X. Y. Zhao, and H. S. Luo, J. Electron. Mater., **40**, 92 (2011).
[8]S. J. Zhang, J. Luo, W. Hackenberger, N. P. Sherlock, R. J. Meyer, Jr., and T. R. Shrout, J. Appl. Phys. **105**, 104506 (2009).
[9]Z. R. Li, X. Xu, X. Yao, Z. and Y. Cheng, J. Appl. Phys. **104**, 024112 (2008).
[10]F. Fang, W. Yang, and X. Luo, J. Am. Ceram. Soc. **93**, 3916 (2010).
[11]R. Zhang, B. Jiang, W. H. Jiang, and W. W. Cao, Appl. Phys. Lett. **89**, 242908 (2006).
[12]S. Zhang, S. Lee, D. Kim, H. Lee, and T. Shrout, J. Am. Ceram. Soc. **90**, 3859 (2007).
[13]F. Wang, J. Luo, D. Zhou, X. Zhao, and H. Luo, Appl. Phys. Lett. **90**, 212903 (2007).
[14]S. J. Zhang, F. Li, J. Luo, R. Xia, W. Hackenberger, and T. R. Shrout, Appl. Phys. Lett. **97**, 132903 (2010).
[15]F. Li, S. Zhang, Z. Xu, X. Wei, J. Luo, and T. Shrout, Appl. Phys. Lett. **97**, 252903 (2010).
[16]E. Sun, S. Zhang, J. Luo, T. Shrout, and W. Cao, Appl. Phys. Lett. **97**, 032902 (2010).
[17]S. J. Zhang, J. Luo, F. Li, R. J. Meyer, Jr., W. Hackenberger, and T. R. Shrout, Acta Mater., **58**, 3773 (2010).
[18]S. Zhang, N. Sherlock, R. Meyer, and T. Shrout, Appl. Phys. Lett. **94**, 162906 (2009).
[19]P. Han, W. Yan, J. Tian, X. Huang, and H. Pan, Appl. Phys. Lett. **86**, 052902 (2005).
[20]R. J. Meyer, Jr., T. M. Tremper, D. C. Markley, D. Van Tol, P. Han, and J. Tian, U.S. Navy Workshop on Acoustic Transduction Materials and Devices, State College, PA, May 2010.
[21]D. J. Van Tol and R. J. Meyer, Jr., "Acoustic Transducer," U.S. patent 7,615,912 Nov. 10, 2009.
[22]S. Zhang, F. Li, W. Jiang, J. Luo, R. Meyer Jr., W. Cao, and T. Shrout, Appl. Phys. Lett. **98**, 182903 (2011).
[23]F. Li, S. Zhang, Z. Xu, X. Wei, and T. Shrout, Ad. Funct. Mater. **21** 2118 (2011).
[24]S. J. Zhang, F. Li, J. Luo, R. Xia, W. Hackenberger, and T. R. Shrout, IEEE Trans. Ultrason. Ferroelectr. Freq. Contr. **58**, 274 (2011).
[25]IRE Standards on Piezoelectric Crystals. Proc. IRE **46**, 764 (1958).
[26]W. P. Mason, *Piezoelectric Crystals and Their Application to Ultrasonics*, (D. Van Nostrand, New York, 1950).
[27]R. Bechmann, Proc. Phys. Soc. (London) **B64**, 323 (1951).
[28]H. Ekstien, Phys. Rev. **66**(5–6) 108 (1944)
[29]M. Kim, J. Kim, and W. W. Cao, J. Appl. Phys. **99**, 074102 (2006).